Adsorption of organic compounds to diesel soot: Frontal analysis and polyparameter linear free energy relationship

Zhijiang Lu*, John MacFarlane and Philip Gschwend

Ralph M. Parsons Laboratory, Department of Civil and Environmental Engineering, Massachusetts Institute of Technology

77 Massachusetts Ave., Cambridge, MA 02139, USA

*Corresponding author phone: (951)-318-5315; fax: (617)258-8850;

E-mail: zhijiang@mit.edu;zhijianglu@gmail.com

Number of pages: 27

Texts: 2

Tables: 5

Figures: 16

Text S1

Polyparameter linear free energy relationship with 4 parameters

It was also possible to fit the ppLFER model well with only 4 parameters (including a constant). With all the 102 measurements, the regression was:

$$\log K_{sootC} = (4.04 \pm 0.12)V + ((-0.30 \pm 0.02)\log a_i)E + (-3.47 \pm 0.13)B + (-1.67 \pm 0.11)$$

(N=102, R^2=0.94, SE=0.22) Equation S1

In general, the same most important parameter were found (compare to Equation 5 in the main text). Again, rigid statistic methods were applied to identify usual points and totally, 6 such points were detected: 1 data point with leverage value larger than limit also with SRE 3.4 (the lowest concentration of atrazine, the blue square in Figure S7); 1 with leverage value larger than limit (the highest concentration of dimethylphthalate, the red triangle in Figure S7) and 4 with SRE between 2 and 3 (the lowest concentration of anisole and nitrobenzene, the second lowest concentration of nitrobenzene and atrazine, green triangles in Figure S7). Removal of these suspicious data points step by step, and rebuilding the ppLFER models gave the following:

Remove 1 data point with leverage value larger than limit also with SRE 3.4

$$\log K_{sootC} = (4.07 \pm 0.11)V + ((-0.31 \pm 0.02)\log a_i)E + (-3.42 \pm 0.12)B + (-1.73 \pm 0.10)$$

(N=101, R^2=0.95, SE=0.20) Equation S2

Remove 2 data point with leverage value larger than limit:

$$\log K_{sootC} = (4.07 \pm 0.11)V + ((-0.31 \pm 0.02)\log a_i)E + (-3.41 \pm 0.12)B + (-1.73 \pm 0.10)$$

(N=100, R^2=0.95, SE=0.20) Equation S3

Remove all 6 suspicious data points:

$$\log K_{sootC} = (4.15 \pm 0.10)V + ((-0.31 \pm 0.02)\log a_i)E + (-3.36 \pm 0.11)B + (-1.82 \pm 0.09)$$

(N=96, R^2=0.96, SE=0.17) Equation S4

Predictions of *log* K_{sootC} values by these models are shown in Figures S8-S10, respectively. Again, there were no significant differences among all these models (Equations S1-3). However, all these models had larger SE compared to 5 parameters ppLFER models. Thus, Equation 5 was suggested to use and when Equation S1 was only suggested when sorbates' *A* parameters were not available.

Text S2

Prediction of Freundlich coefficients and exponents. Freundlich coefficients and exponents can be calculated by combining Equations 3 and 5 [1, 2]:

$$\log K_f((\text{mg kg}^{-1})/(\text{mg L}^{-1})^n) = (3.74 \pm 0.11)V + (-0.62 \pm 0.10)A + (-3.35 \pm 0.11)B - \left((-0.35 \pm 0.02)\log C_{w,sat}\right)E + (-1.45 \pm 0.09) \quad \text{Equation S5}$$

$$n = 1 + (-0.35 \pm 0.02)E \quad \text{Equation S6}$$

where $C_{w,sat}$ is the sorbate (subcooled) liquid solubility in mg L^{-1}. According to these equations, the Freundlich coefficients and exponents of our 21 sorbates were predicted (Figure S11). Predictions of Freundlich coefficients accurately matched measured values (Figure S11a). However, predictions of *n* values were much less accurate (Figure S11b). This may due to using only one parameter (*E* term) to estimate *n* in Equation S6, implying the need to use a wider spectrum of sorbates to isolate the factors that control *n*. It should be noted that the worst case was atrazine with a residue (the difference between the predicted value and the observed value) of 0.34 while residues for other 20 sorbates were smaller than 0.18. Again, this suggests aspects of atrazine's stereochemistry (non-planar or molecular size) are causing such sorbates to deviate from the ppLFER-based expectations.

71 Table S1 Octanol-water partition coefficients and Abraham descriptors of selected sorbates

Compounds	**log K_{OW}**	**V *** (cm^3 mol^{-1})/100	**E*** (cm^3 mol^{-1})/100	**S***	**A***	**B***
trichloroethene	2.42	0.715	0.52	0.37	0.08	0.03
benzene	2.17	0.716	0.61	0.52	0	0.14
acetophenone	1.63	1.014	0.82	1.01	0	0.48
aniline	0.95	0.816	0.96	0.96	0.26	0.41
anisole	2.11	0.916	0.71	0.75	0	0.29
toluene	2.69	0.857	0.6	0.52	0	0.14
fluorobenzene	2.24	0.734	0.477	0.57	0	0.1
chlorobenzene	2.78	0.839	0.72	0.65	0	0.07
1,2,4-trichlorobenzene	4.06	1.084	0.98	0.81	0	0
bromobenzene	2.99	0.891	0.882	0.73	0	0.09
nitrobenzene	1.85	0.891	0.871	1.11	0	0.28
2,4-dinitrotoluene	2	1.21	1.17	1.48	0.05	0.45
phenol	1.44	0.775	0.81	0.89	0.6	0.3
4-chlorophenol	2.42	0.898	0.92	1.08	0.67	0.21
4-cresol	1.93	0.92	0.82	0.87	0.57	0.31
naphthalene	3.33	1.085	1.34	0.92	0	0.2
1-methylnaphthalene	3.87	1.226	1.34	0.94	0	0.22
1-chloronaphthalene	4	1.21	1.42	1	0	0.14
dimethylphthalate	1.53	1.43	0.78	1.4	0	0.86
atrazine	2.65	1.62	1.51	1.29	0.17	1.01
phenanthrene	4.46	1.454	2.06	1.29	0	0.26

72 * Data from UFZ-LSER database [3]

73

Table S2 Pearson correlation of ppLFER parameters (N=21).

		E	S	A	B
V	Pearson Correlation	0.78*	0.78*	-0.21	0.66*#
	Sig. (2-tailed)	0.00	0.00	0.36	0.00
E	Pearson Correlation		0.64*	-0.09	0.26
	Sig. (2-tailed)		0.00	0.71	0.25
S	Pearson Correlation			0.10	0.71*
	Sig. (2-tailed)			0.66	0.00
A	Pearson Correlation				0.10
	Sig. (2-tailed)				0.65

*. Correlation is significant at the 0.01 level (2-tailed).

#. Correlation is not significant after removing dimethylphthalate and atrazine (correlation coefficient 0.24, 2-tailed significance 0.332)

Table S3 Comparisons of reported Freundlich isotherm parameters of selected sorbates on soot, char, and activated carbon by different methods.

Sorbate	Sorbent	Method	$log\ K_f$	n	Ref.
benzene	NIST soot 2975	frontal analysis, 4hr	1.37	0.71	This study
	chestnut wood char	batch, 14 d	3.08	0.75	Plata et al.[2]
	granular activated carbon	batch, 14 d	4.50	0.29	Shih and Gschwend[1]
toluene	NIST soot 2975	frontal analysis, 4 hr	1.72	0.79	This study
	chestnut wood char	batch, 14 d	3.21	0.79	Plata et al.[2]
	granular activated carbon	batch, 14 d	4.80	0.30	Shih and Gschwend[1]
nitrobenzene	NIST soot 2975	frontal analysis, 6 hr	2.22	0.51	This study
	chestnut wood char	batch, 14 d	3.74	0.46	Plata et al.[2]
	granular activated carbon	batch, 14 d	4.88	0.19	Shih and Gschwend[1]
naphthalene	NIST soot 2975	frontal analysis, 8 hr	2.80	0.55	This study
	NIST soot 2975	batch, 28 d	3.21	0.60	Endo et al.[4]
	NIST soot 2975/methanol extracted	batch, 28 d	3.29	0.41	Endo et al.[4]
1,2,4-trichlorobenzene	NIST soot 2975	frontal analysis, 6 hr	3.06	0.54	This study
	NIST soot 2975	batch, flocculation, 59 d	3.43	0.66	Nguyen et al.[5]
	NIST soot 2975	batch, 60 d	3.42	0.66	Nguyen and Ball[6]
	NIST soot 1650b	batch, 60 d	3.80	0.82	Nguyen and Ball[6]
	oxidized hexane soot	batch, 60 d	3.53	0.67	Nguyen and Ball[6]
phenanthrene	NIST soot 2975	frontal analysis, 33 hr	3.54	0.31	This study
	NIST soot 2975	batch, flocculation, 59 d	3.68	0.43	Nguyen et al.[5]
	NIST 1650	air-bridge, 134 d	5.37	1	Bucheli and Gustafsson[7]
	375 ºC combusted Lake Ketelmeer sediment	batch POM-SPE, 35 d	4.24	0.54	Cornelissen and Gustafsson[8]
	NIST soot 2975	batch, 60 d	3.72	0.41	Nguyen and Ball[6]
	NIST soot 1650b	batch, 60 d	3.58	0.6	Nguyen and Ball[6]
	hexane soot	batch, 60 d	3.64	0.52	Nguyen and Ball[6]
	oxidized hexane soot	batch, 60 d	3.48	0.52	Nguyen and Ball[6]
atrazine	NIST soot 2975	frontal analysis, 10 hr	2.37	0.81	This study
	375 ºC combusted Lake Ketelmeer sediment	batch POM-SPE, 35d	3.01	0.97	Cornelissen and Gustafsson[8]
4-chlorophenol	NIST soot 2975	frontal analysis, 13 hr	2.35	0.62	This study
	carbon black	batch, 1 d	3.50	0.4	Shih et al.[9]
	rice straw char	batch, 1 d	3.11	0.56	Shih et al.[9]

Table S4 Octanol-water partition coefficients, subcooled liquid solubilities, and Abraham descriptors of selected PAHs and PCBs

Compounds	**log K_{OW}**	**subcooled liquid solubility* µg L^{-1}**	**V[#]**	**E[#]**	**S[#]**	**A[#]**	**B[#]**
fluorene	4.14	11397	1.357	1.59	1.06	0	0.25
anthracene	4.45	5100	1.454	2.29	1.34	0	0.28
fluoranthene	5.16	1207	1.585	2.38	1.55	0	0.24
pyrene	4.88	1119	1.585	2.81	1.71	0	0.28
chrysene	5.73	133	1.823	3.03	1.73	0	0.33
benz[a]anthracene	5.79	135	1.823	2.99	1.7	0	0.33
benzo[b]fluoranthene	6.6	19.62	1.954	3.19	1.82	0	0.4
benzo[k]fluoranthene	6.84	128	1.954	3.19	1.91	0	0.33
benzo[a]pyrene	6.13	13.56	1.954	3.63	1.98	0	0.44
dibenz[a,h]anthracene	6.75	737	2.192	4	2.04	0	0.44
PCB44	5.8	164	1.8138	1.9	1.48	0	0.15
PCB66	6.2	381	1.8138	1.91	1.46	0	0.13
PCB101	6.4	322	1.9362	2.04	1.61	0	0.13
PCB153	6.9	5.88	2.0586	2.18	1.74	0	0.11
PCB138	6.83	12.79	2.0586	2.18	1.74	0	0.11
PCB180	7.72	3.73	2.181	2.29	1.87	0	0.09
PCB170	7.36	3.73	2.181	2.33	1.87	0	0.09

***** Data from van Noort[10], Shiu and Mackay[11] and Liu et al.[12]

[#] Data from Abraham and Al-Hussaini[13] and UFZ-LSER database.[3]

Table S5 Comparisons of reported ppLFER models for adsorption to soot, char, carbon nanotube and activated carbon.

Sorbent	ppLFER model	N	R^2	SE	Ref
NIST soot 2975	$\log K_{sootC} = (3.74\pm0.11)V + ((-0.35\pm0.02)\log a_i)E + (-0.62\pm0.10)A + (-3.35\pm0.11)B + (-1.45\pm0.09)$	102	0.96	0.18	This study
Chestnut wood char	$\log K_d = ((4.03 \pm 0.14) + (-0.15 \pm 0.04) \log a_i))V + ((-0.28 \pm 0.04) \log a_i))S + (-5.20 \pm 0.21)B$	128	0.98	0.41	Plata et al.[2]
MWCNT	$\log K=f_1+f_2E+f_3S+f_4A+f_5B+f_6V$ $f_1=0.528(\log a_i)^2+ 1.23\log a_i - 4.25;$ $f_2= 0.0204(\log a_i)^2 + 0.265\log a_i+ 0.229;$ $f_3 = 0.0644(\log a_i)^2 + 0.118\log_i + 0.849;$ $f_4=-0.207(\log a_i)^2 - 0.934\log a_i - 2.84;$ $f_5=-0.589(\log a_i)^2 - 1.58\log a_i - 4.04;$ $f_6=-0.450 (\log a_i)^2 - 1.74\log a_i + 3.85$				Zhao et al.[14]
MWCNT	$\log K_{d,\infty} =-(4.31\pm0.37)-(0.01\pm0.21)A-(1.91\pm0.39)B +(4.45\pm0.38)V+(1.06\pm0.21)S$	58	0.83		Apul et al.[15]
	$\text{Log } K_{d,\ 0.01}=-(3.81\pm0.78)-(1.31\pm0.56)A-(2.86\pm1.22)B+(4.41\pm0.70)V+(0.67\pm0.47)S$	20	0.85		
	$\log K_{d,\ 0.1}=-(4.42\pm0.55)B-(1.29\pm0.40)A-(3.81\pm0.85)B+(4.59\pm0.49)V+(0.74\pm0.33)S$	20	0.93		
GAC	$\log K_d= ((3.76 \pm 0.28) + (-0.20 \pm 0.10) \log a_i))V +((-0.80 \pm 0.14) +(-0.48 \pm 0.05)\log a_i))S+ ((-4.47 \pm 0.20) +(-0.16 \pm 0.06) \log a_i))B + (0.73 \pm 0.28) - (0.24 \pm 0.09) \log a_i$	176	0.96		Shih and Gschwend[1]
GAC	$\log K_{d,\infty} = (4.29 \pm 0.12)V +(0.92 \pm 0.49)E + (0.42 \pm 0.13)S - (0.20 \pm 0.11)A - (2.93\pm 0.74)B - (2.25\pm 0.32)$	22	0.96	0.07	Poole and Poole[16]
GAC	$\log K_{d,\infty} = 3.35V - 1.14B - D^*$	360	0.846	0.65	Luehrs et al.[17]
GAC	$\log K_{d,\infty} = 3.06V + 0.56S - 3.20B - 1.93$	37	0.974	0.19	Kamlet et al.[18]

*D accounts for differences in data sets.

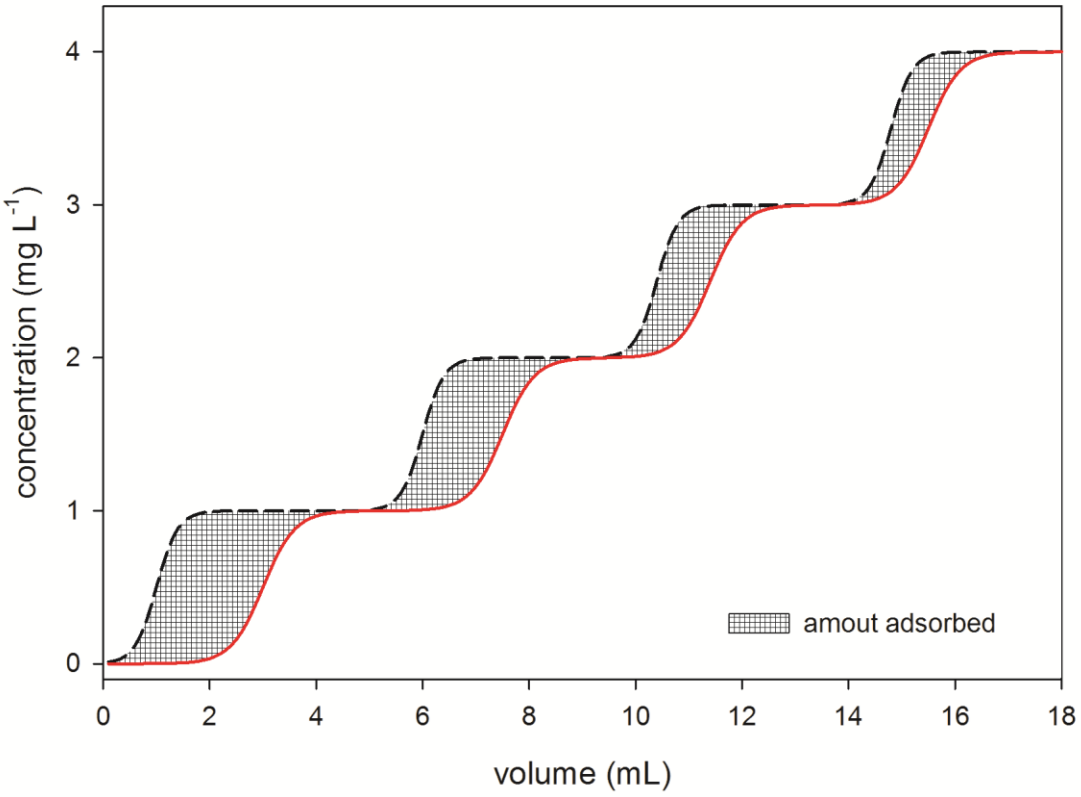

Figure S1 Illustration of breakthrough of stair-case frontal analysis

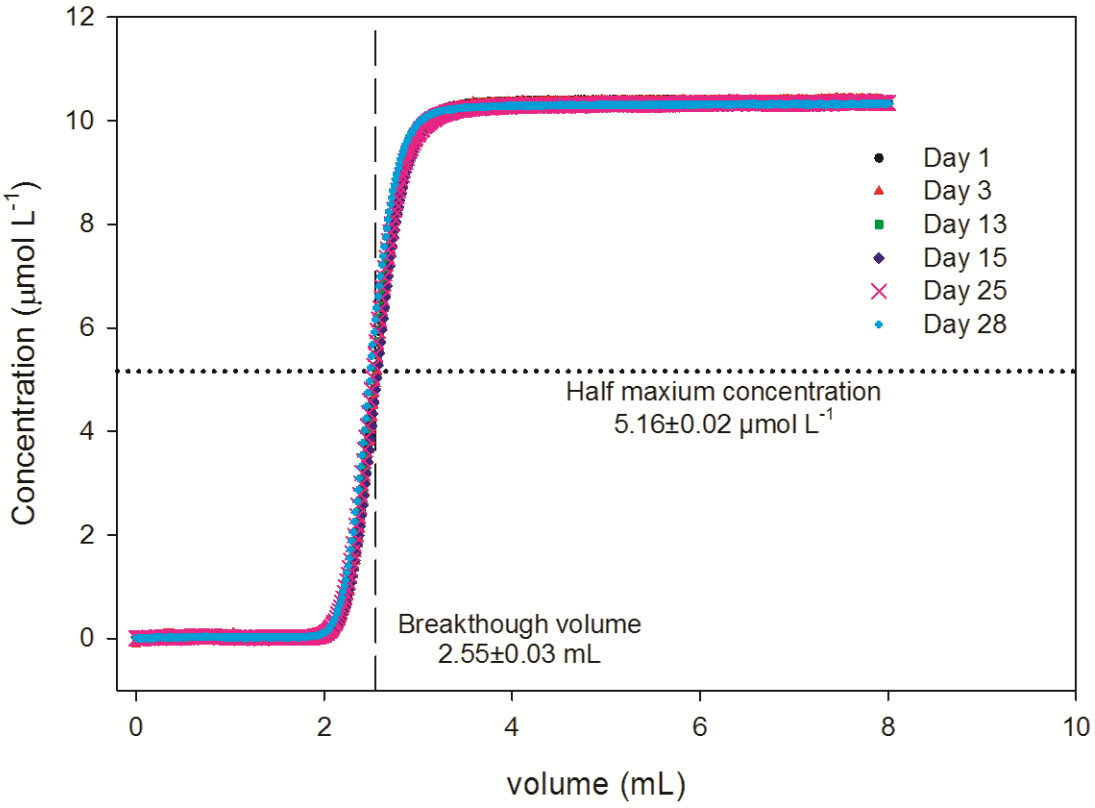

Figure S2 Nitrate breakthrough curves on 1% soot column within a month.

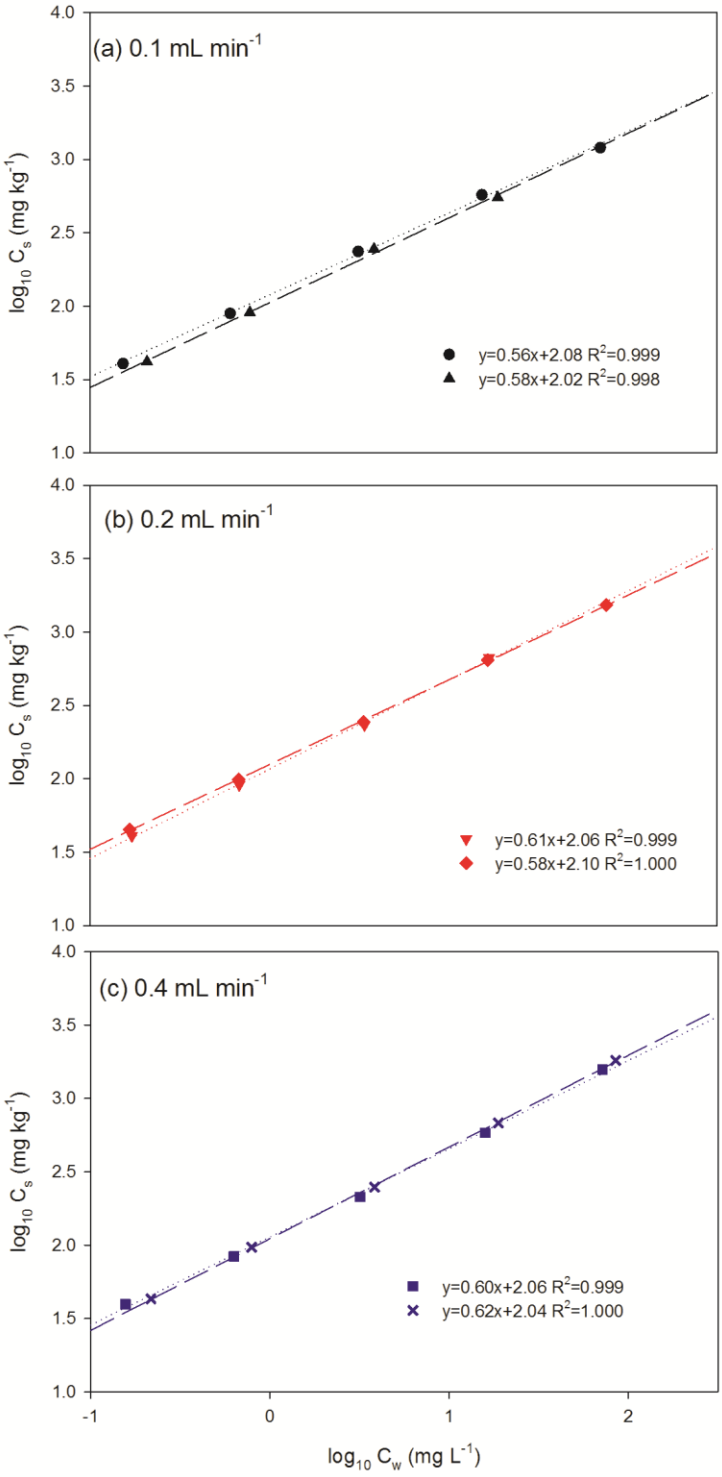

Figure S3 Isotherms of anisole at different flow rates obtained on 1% soot column: (a) at 0.1 mL min^{-1}; (b) at 0.2 mL min^{-1}; and (c) at 0.4 mL min^{-1}.

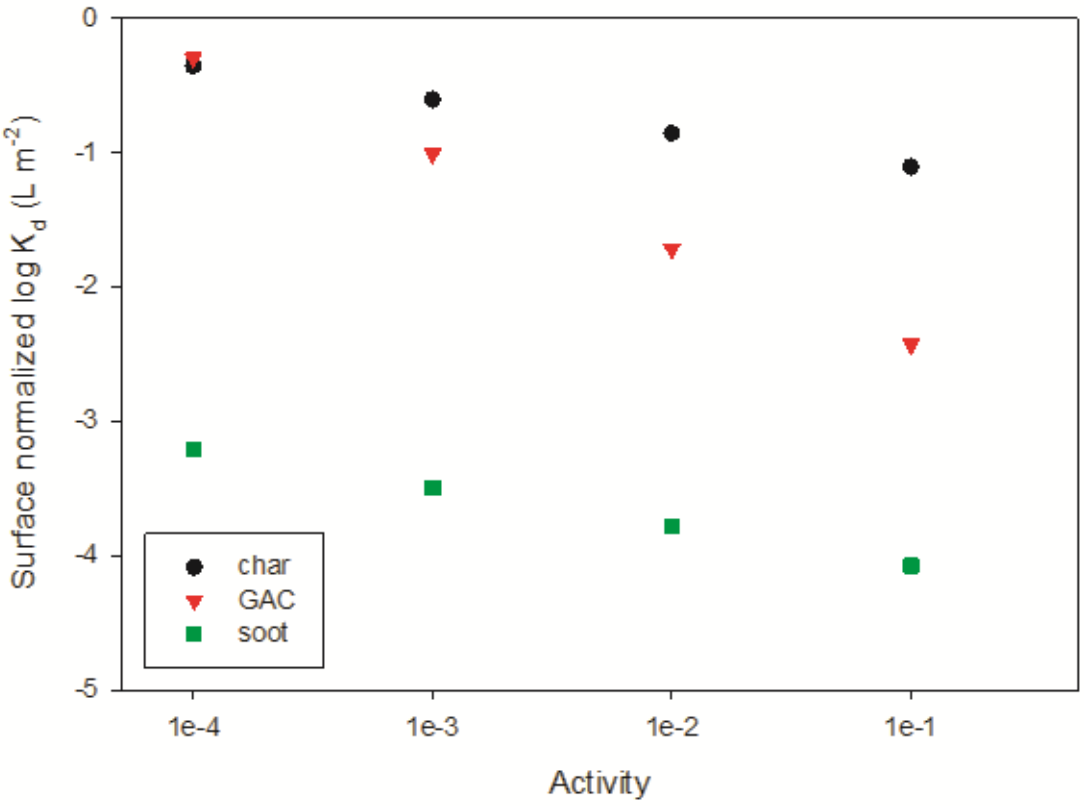

Figure S4 Surface-area normalized adsorption coefficients of benzene on char (5.9 m^2 g^{-1}), granular activated carbon (556 m^2 g^{-1}), and soot (91 m^2 g^{-1}). Data from this study from Shih and Gschwend, and Plata et al.[1, 2]

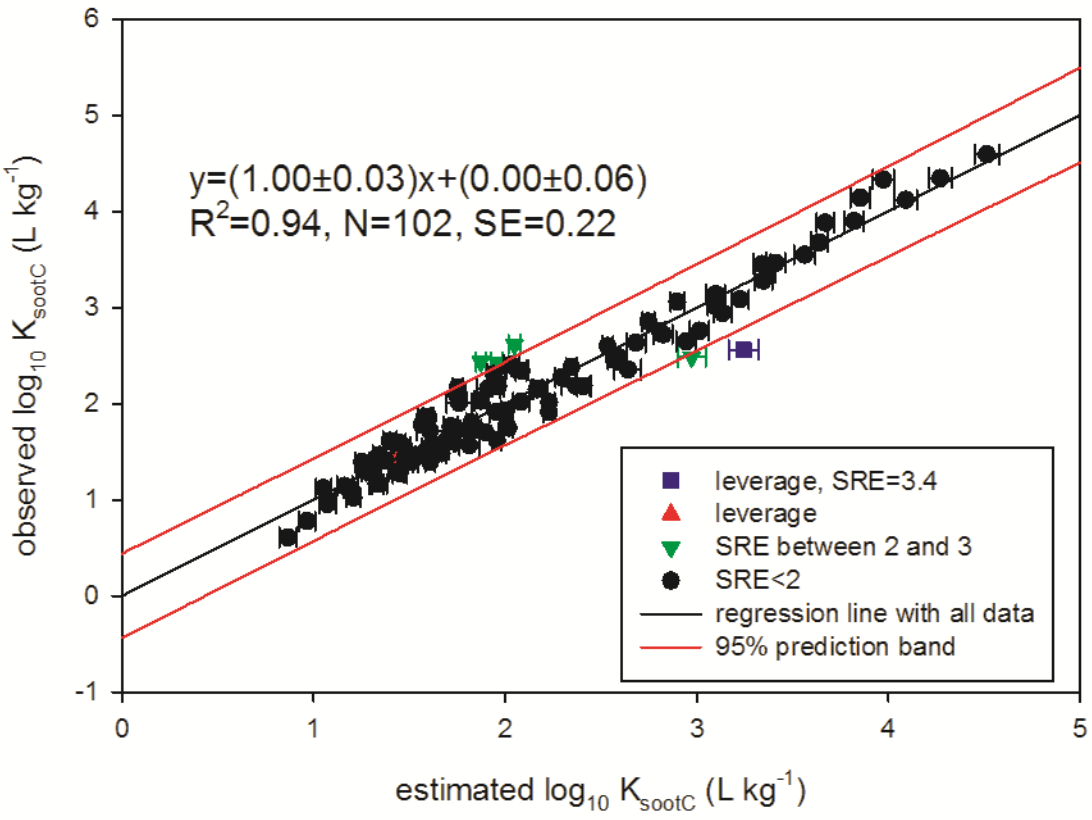

Figure S5 Prediction of *log K_{sootC}* by the 4 parameters ppLFER models with all data (Equation S1). Error bars in the horizontal reflect propagated errors using uncertainties in the fitted ppLFER coefficients.

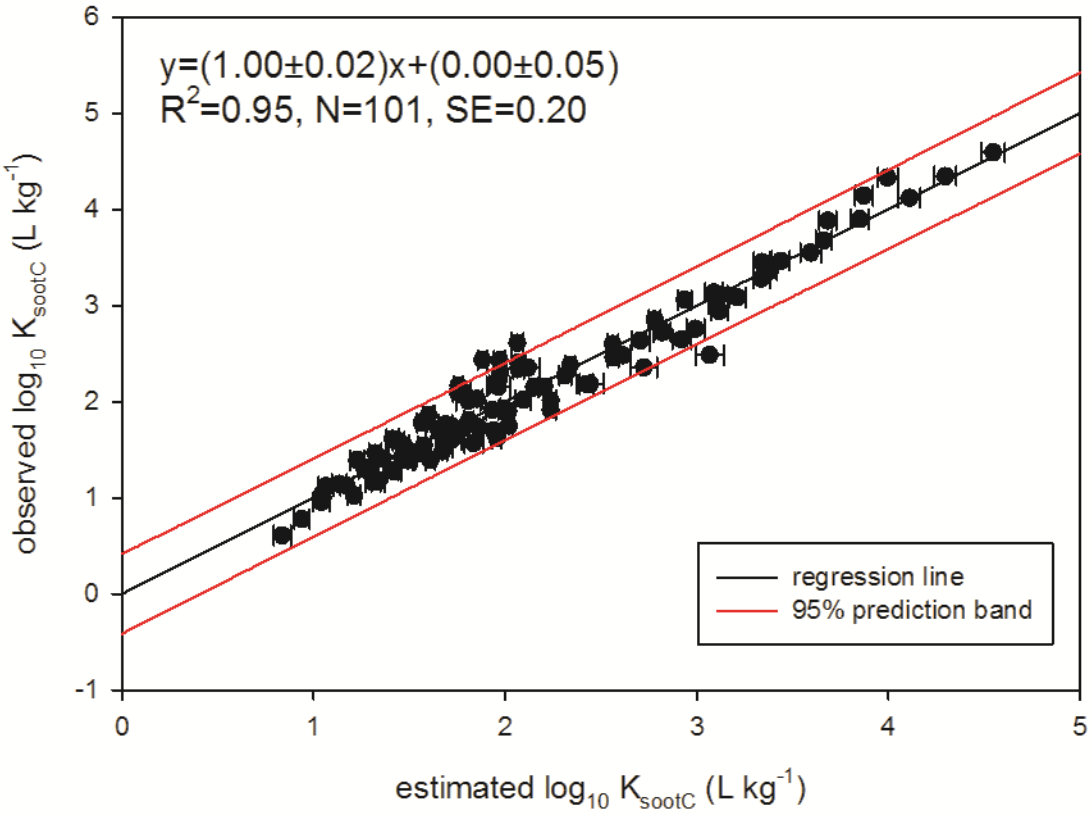

123

124 Figure S6 Prediction of *log* K_{sootC} by the 4 parameter ppLFER models with 101 data points (Equation
125 S2). Error bars in the horizontal reflect propagated errors using uncertainties in the fitted ppLFER
126 coefficients.

127

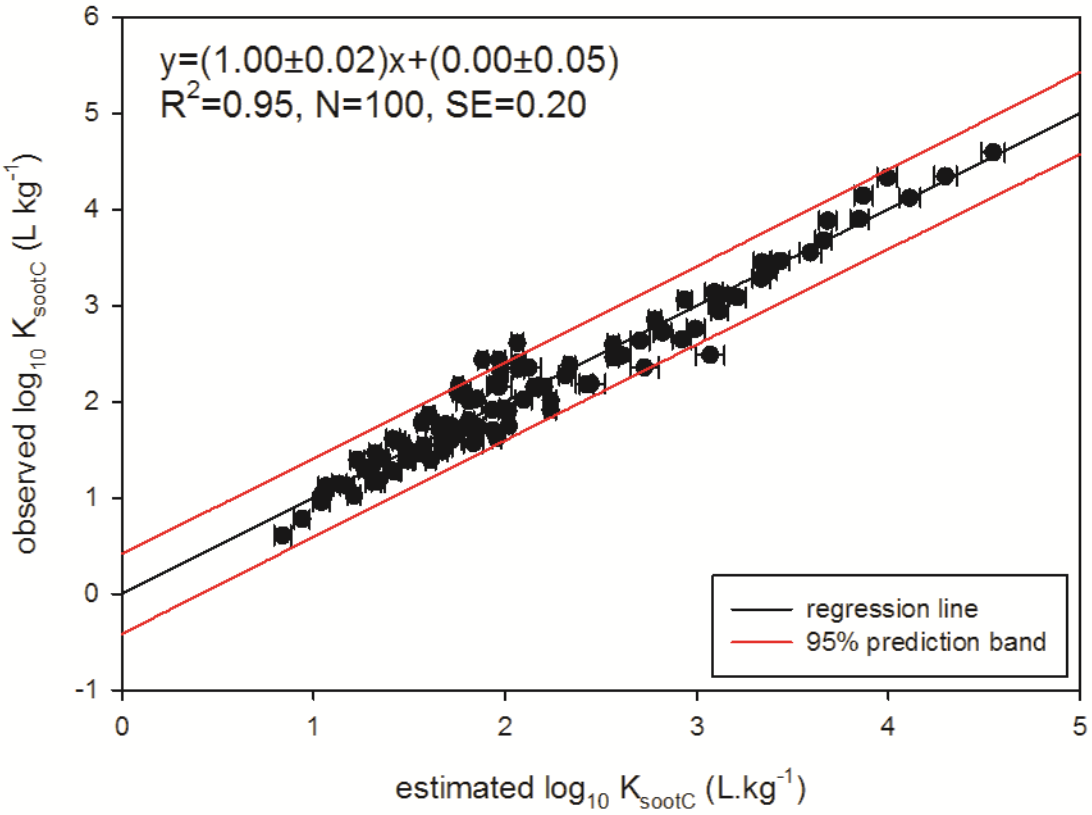

Figure S7 Prediction of *log* K_{sootC} by the 4 parameters ppLFER models with 100 data points (Equation S3). Error bars in the horizontal reflect propagated errors using uncertainties in the fitted ppLFER coefficients.

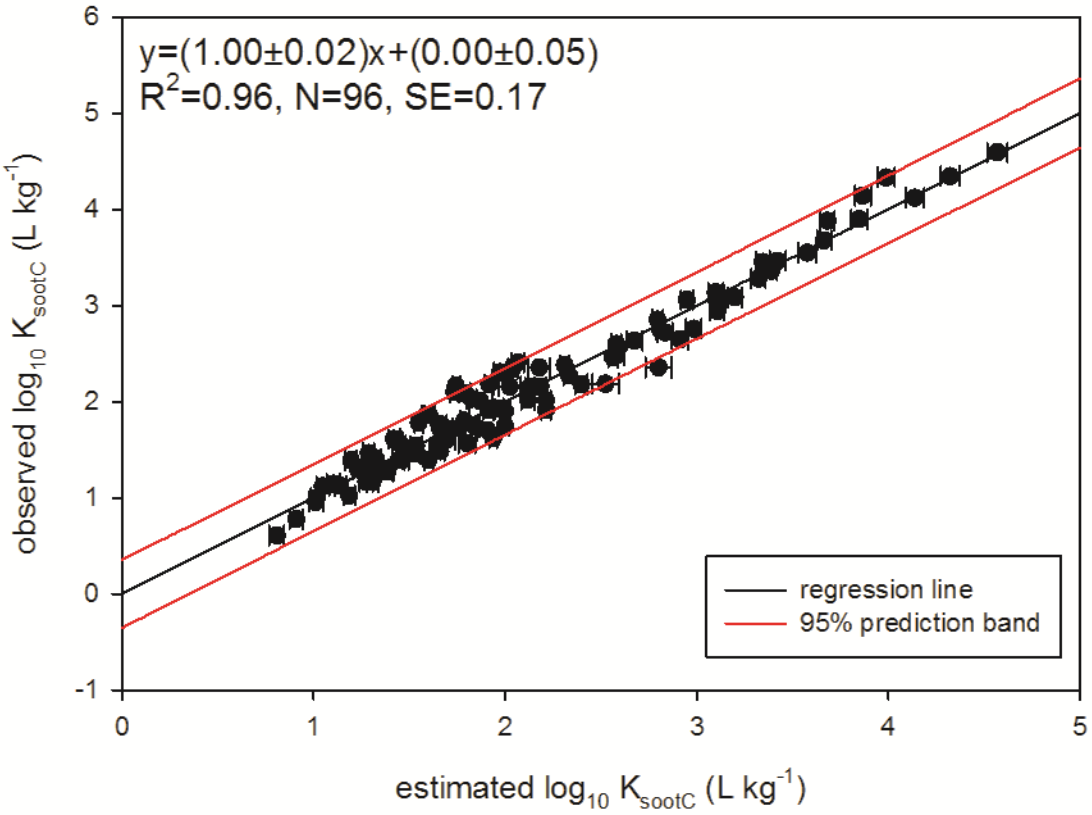

Figure S8 Prediction of *log* K_{sootC} by the 4 parameters ppLFER models with 96 data points (Equation S4). Error bars in the horizontal reflect propagated errors using uncertainties in the fitted ppLFER coefficients.

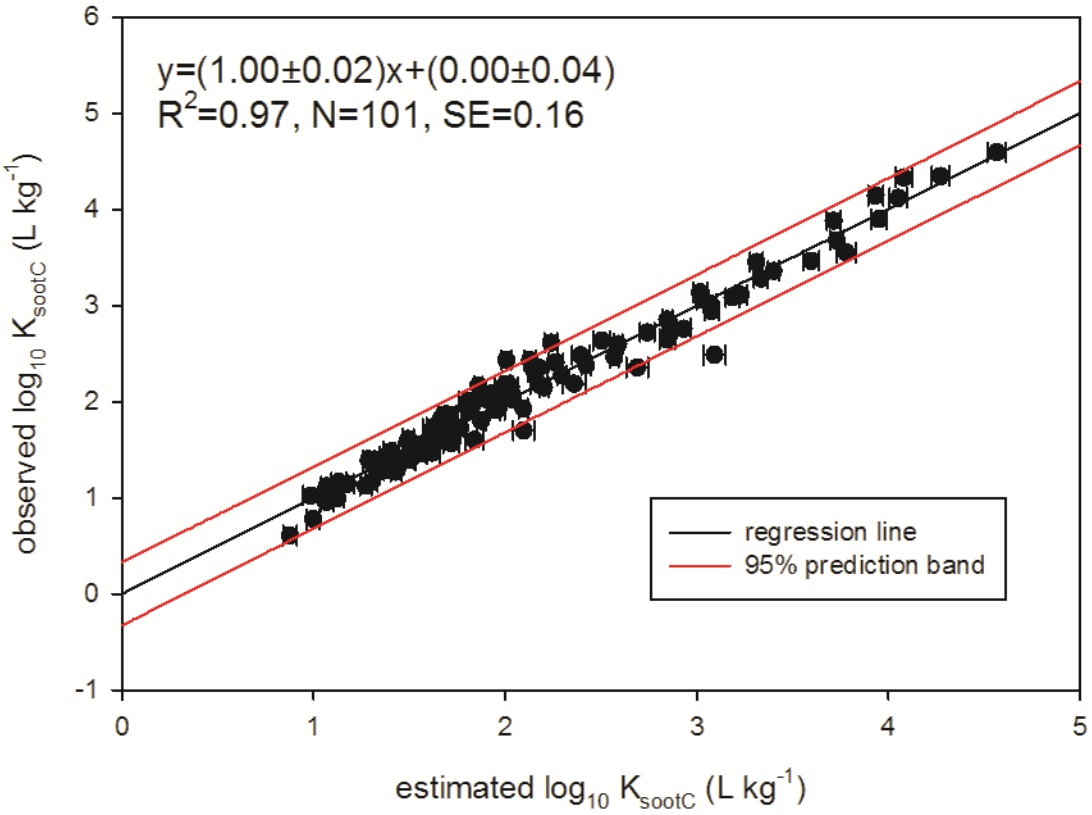

139

140

141 Figure S9 Prediction of *log* K_{sootC} by the ppLFER models excluding the data point SRE 4.5 (Equation
142 6). Error bars in the horizontal reflect propagated errors using uncertainties in the fitted ppLFER
143 coefficients.

144

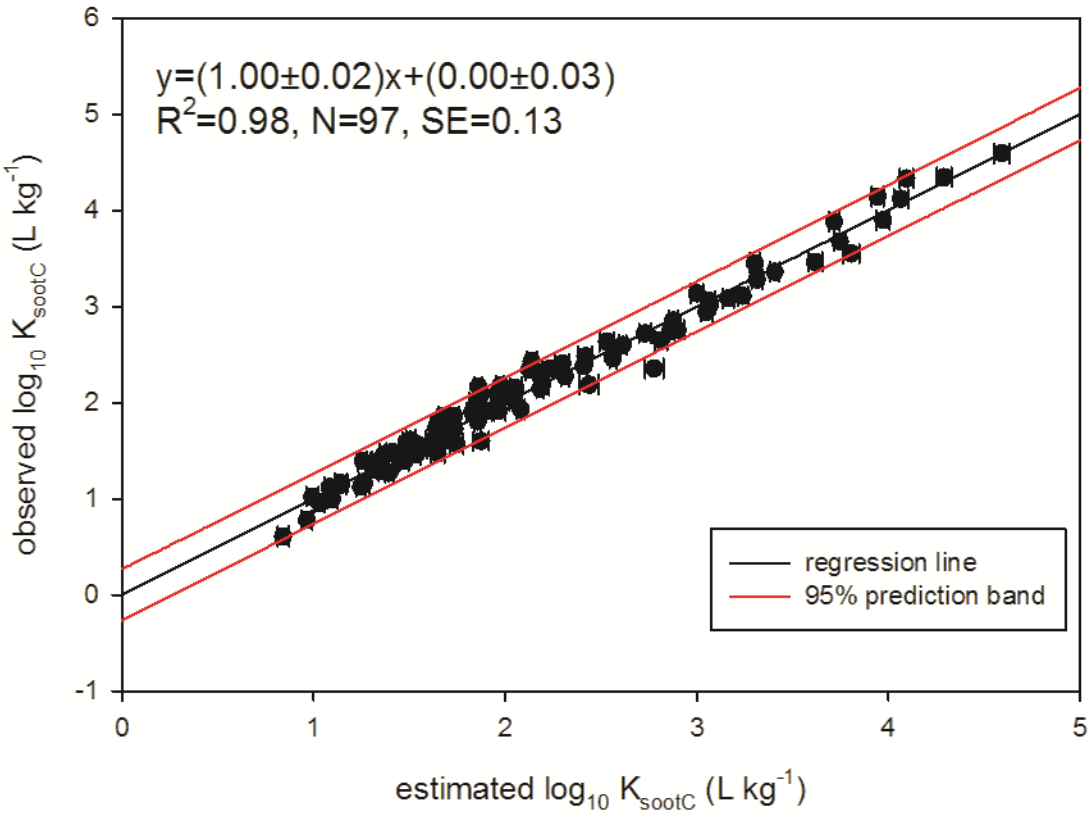

Figure S10 Prediction of *log K_{sootC}* by the ppLFER models excluding five data point SRE > 3 (Equation 7). Error bars in the horizontal reflect propagated errors using uncertainties in the fitted ppLFER coefficients.

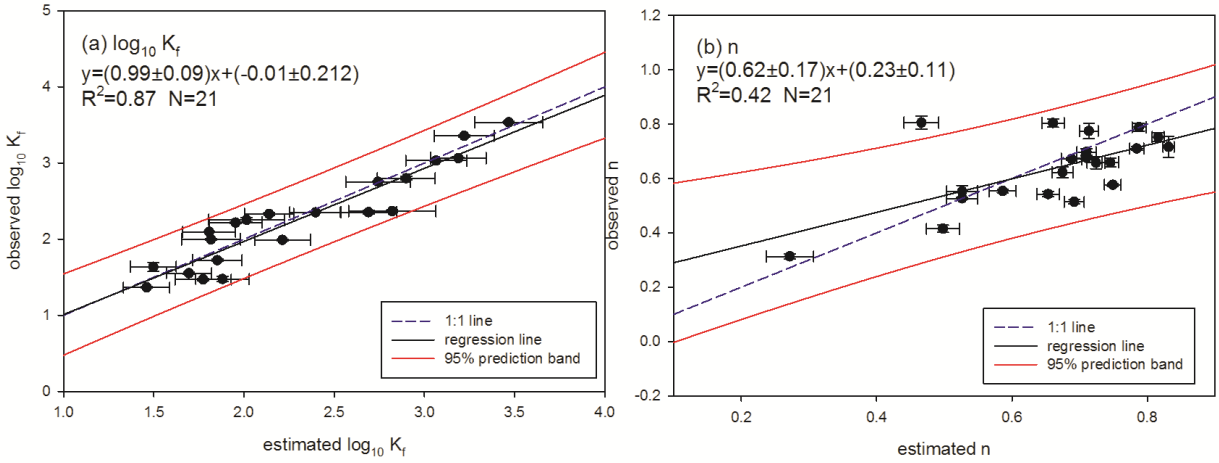

Figure S11 Prediction of (a) Freundlich coefficients and (b) exponents (Equations S5 and 6, respectively). Error bars in the horizontal reflect propagated errors using uncertainties in the fitted ppLFER coefficients. Error bars in the vertical reflect 1 standard error of observed values.

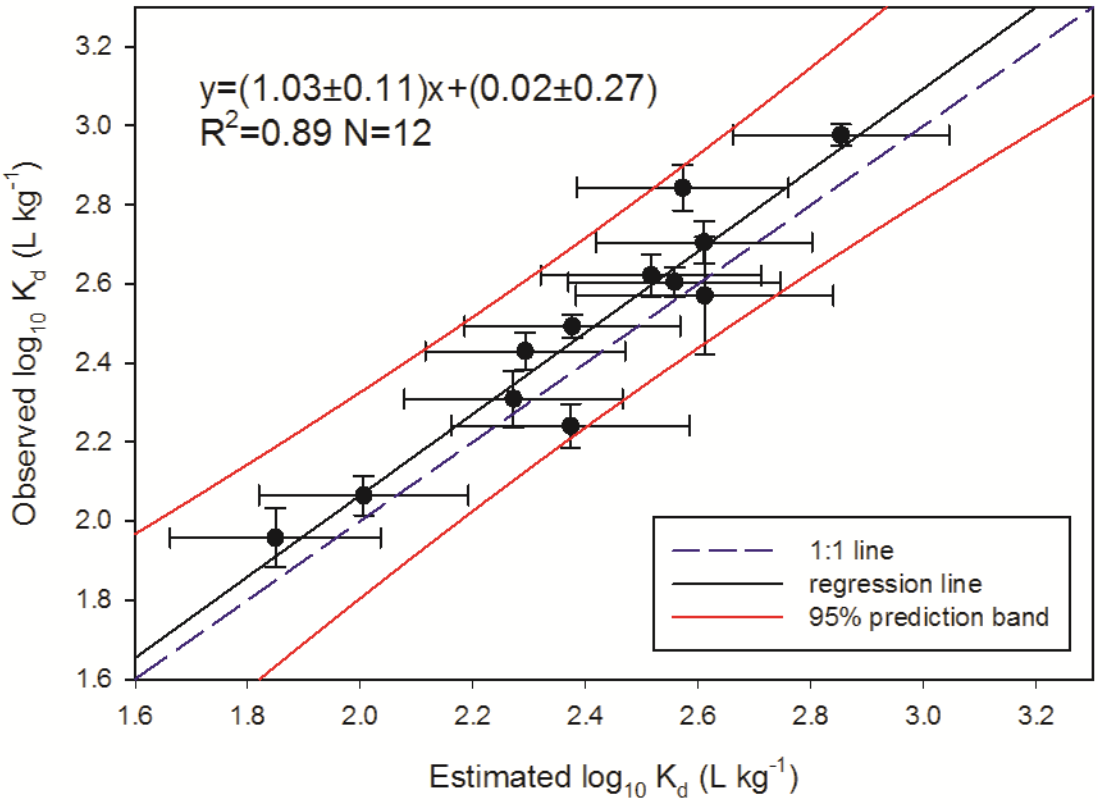

Figure S12 Observed and predicted *log* K_d values of phenanthrene at 100 µg L^{-1} on different EPA soils and sediments. Data from Huang et al.[19] and Accardi-Dey and Gschwend[20]. Error bars in the horizontal reflect propagated errors using uncertainties in the fitted ppLFER coefficients. Error bars in the vertical reflect 1 standard error of observed values.

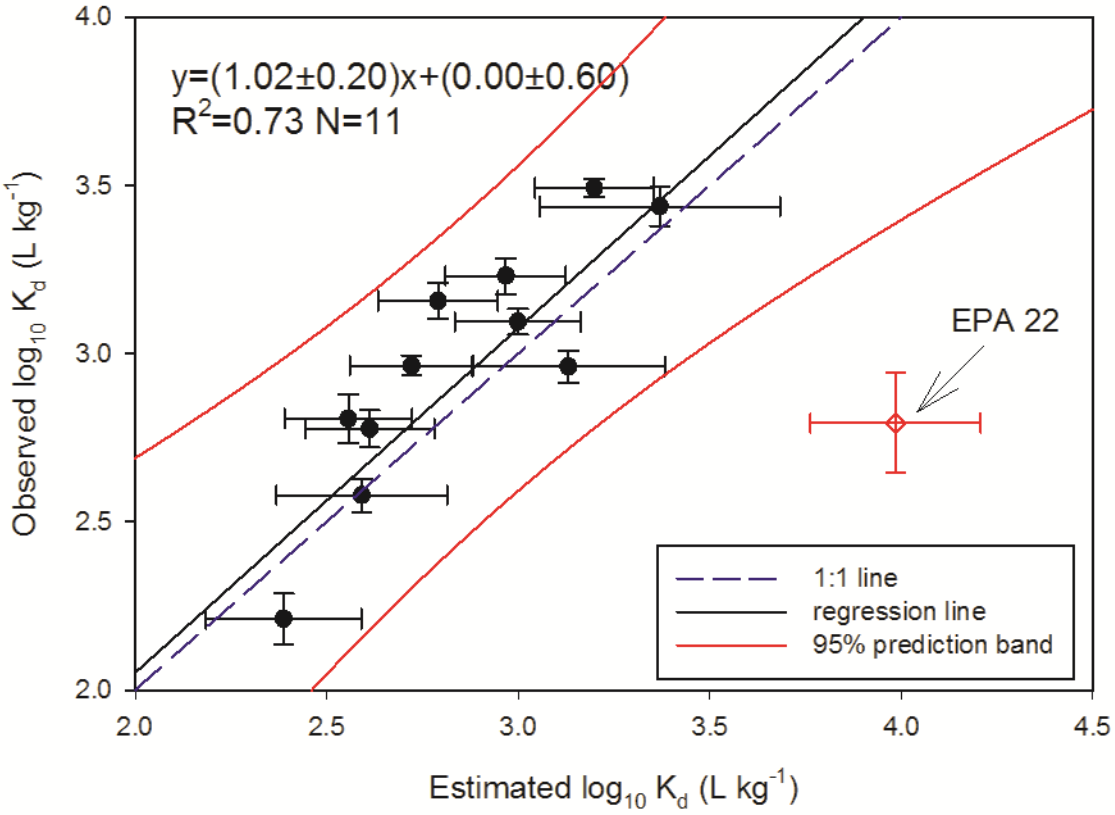

166

167 Figure S13 Observed and predicted *log K_d* values of phenanthrene at 1 µg L^{-1} on different EPA soils and
168 sediments. Data from Huang et al.[19] and Accardi-Dey and Gschwend.[20] Regression does not include EPA
169 22 sediment. Error bars in the horizontal reflect propagated errors using uncertainties in the fitted
170 ppLFER coefficients. Error bars in the vertical reflect 1 standard error of observed values.

171

172

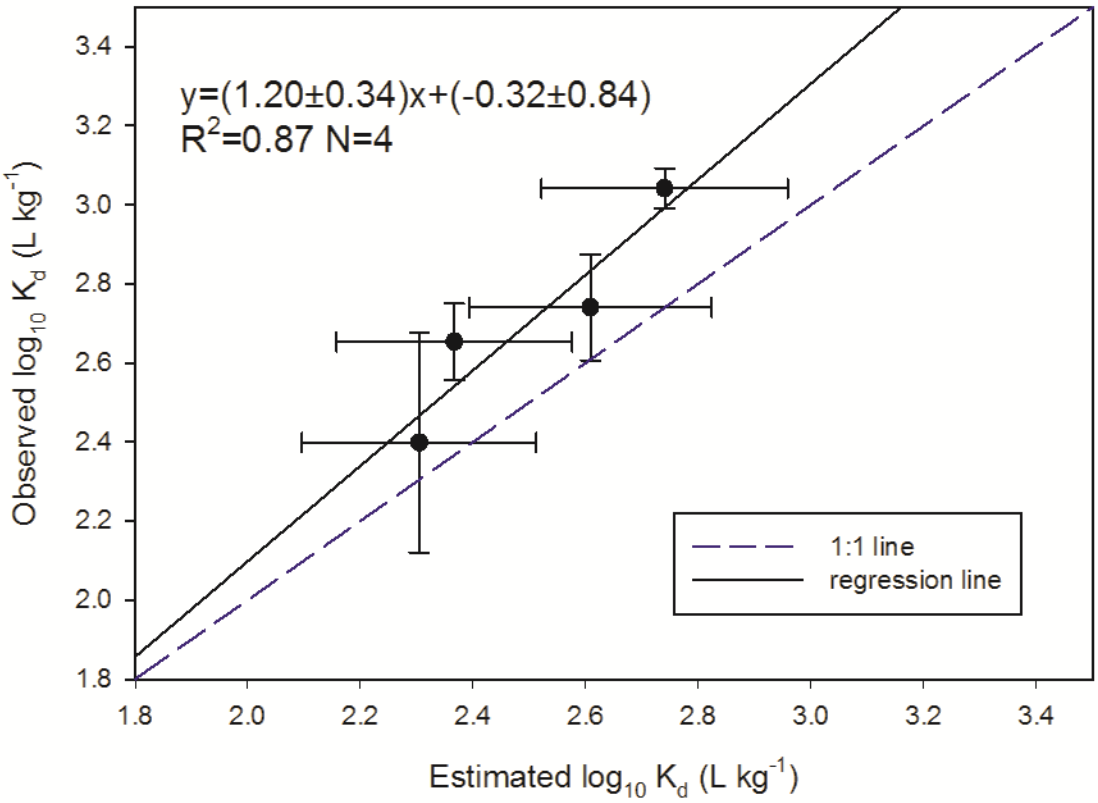

Figure S14 Observed and predicted *log K_d* of phenanthrene on the combusted Boston Harbor sediment. Data from Accardi-Dey and Gschwend[20]. Error bars in the horizontal reflect propagated errors using uncertainties in the fitted ppLFER coefficients. Error bars in the vertical reflect 1 standard error of observed values.

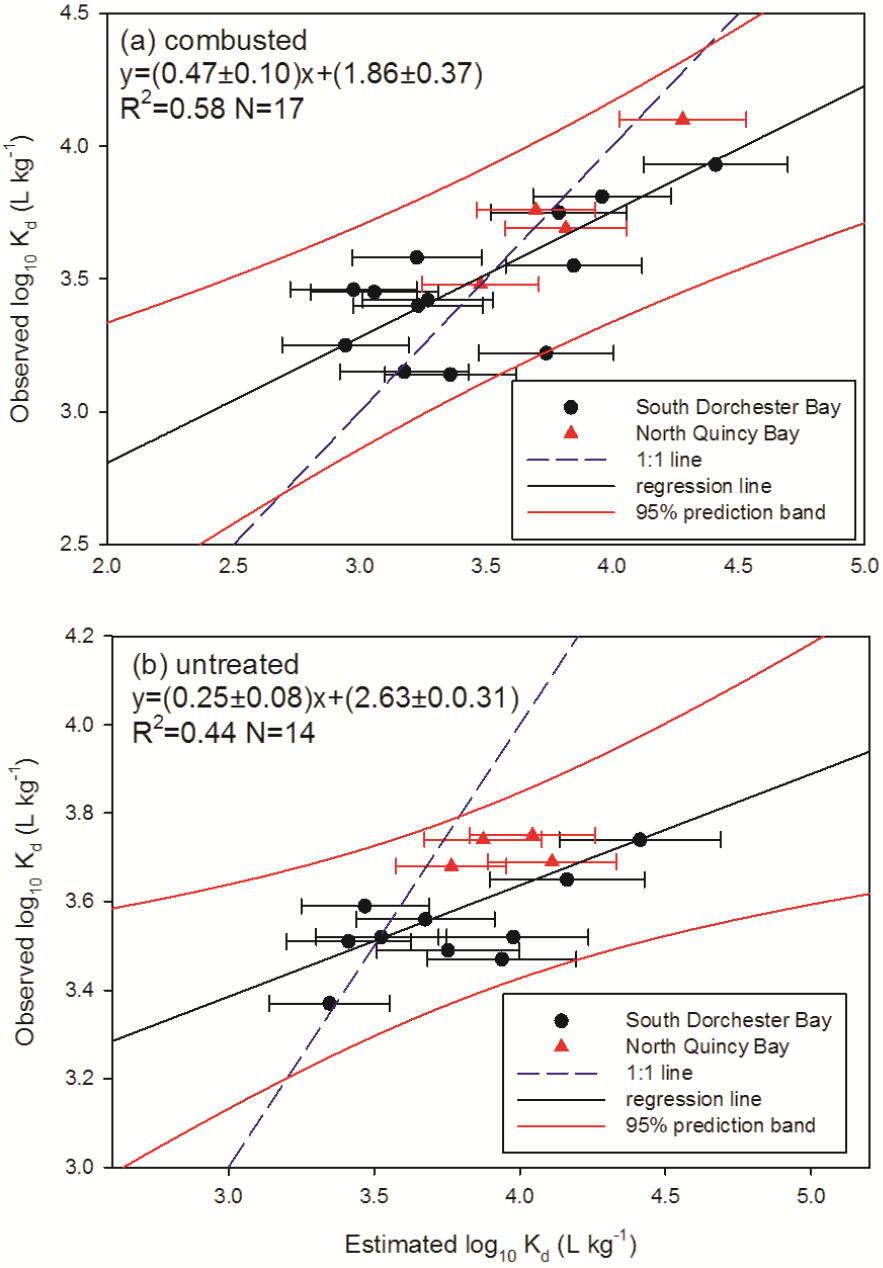

182

183 Figure S15 Observed and predicted *log* K_d of pyrene on the (a) combusted and (b) untreated
184 South Dorchester Bay and North Quincy Bay sediments. Data from Accardi-Dey and Gschwend[21]. Error
185 bars in the horizontal reflect propagated errors using uncertainties in the fitted ppLFER coefficients. Error
186 bars in the vertical reflect 1 standard error of observed values.

187

188

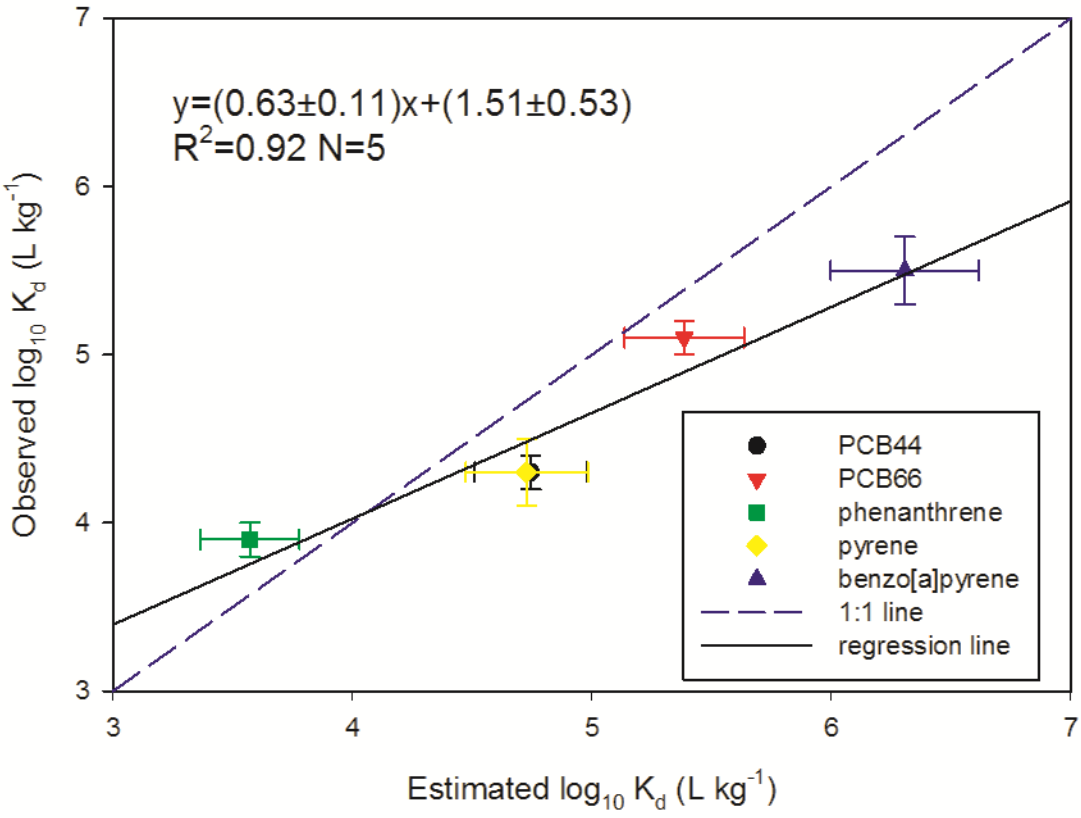

Figure S16 Observed and predicted *log K_d* of PAHs and PCBs on the Boston Harbor sediment. Data from Lohmann et al.[22] Error bars in the horizontal reflect propagated errors using uncertainties in the fitted ppLFER coefficients. Error bars in the vertical reflect 1 standard error of observed values.

References

1. Shih, Y. H.; Gschwend, P. M., Evaluating activated carbon-water sorption coefficients of organic compounds using a linear solvation energy relationship approach and sorbate chemical activities. *Environ. Sci. Technol.* **2009,** *43*, (3), 851-857.

2. Plata, D. L.; Hemingway, J. D.; Gschwend, P. M., Polyparameter linear free energy relationship for wood char-water sorption coefficients of organic sorbates. *Environ. Toxicol. Chem.* **2015,** *34*, (7), 1464-71.

3. UFZ, UFZ-LSER database. http://www.ufz.de/index.php?en=31698&contentonly=1&lserd_data[mvc]=Public/start

4. Endo, S.; Grathwohl, P.; Haderlein, S. B.; Schmidt, T. C., Effects of native organic material and water on sorption properties of reference diesel soot. *Environ. Sci. Technol.* **2009,** *43*, (9), 3187-93.

5. Nguyen, T. H.; Sabbah, I.; Ball, W. P., Sorption nonlinearity for organic contaminants with diesel soot: Method development and isotherm interpretation. *Environ. Sci. Technol.* **2004,** *38*, (13), 3595-3603.

6. Nguyen, T. H.; Ball, W. P., Absorption and adsorption of hydrophobic organic contaminants to diesel and hexane soot. *Environ. Sci. Technol.* **2006,** *40*, (9), 2958-2964.

7. Bucheli, T. D.; Gustafsson, O., Quantification of the soot-water distribution coefficient of PAHs provides mechanistic basis for enhanced sorption observations. *Environ. Sci. Technol.* **2000,** *34*, (24), 5144-5151.

8. Cornelissen, G.; Gustafsson, O., Sorption of phenanthrene to environmental black carbon in sediment with and without organic matter and native sorbates. *Environ. Sci. Technol.* **2004,** *38*, (1), 148-155.

9. Shih, Y.-h.; Su, Y.-f.; Ho, R.-y.; Su, P.-h.; Yang, C.-y., Distinctive sorption mechanisms of 4-chlorophenol with black carbons as elucidated by different pH. *Sci. Total Environ.* **2012,** *433*, 523-529.

10. van Noort, P. C. M., Estimation of amorphous organic carbon/water partition coefficients, subcooled liquid aqueous solubilities, and n-octanol/water partition coefficients of nonpolar chlorinated aromatic compounds from chlorine fragment constants. *Chemosphere* **2009,** *74*, (8), 1024-1030.

11. Shiu, W. Y.; Mackay, D., A critical review of aqueous solubilities, vapor pressures, Henry's law constants, and octanol–water partition coefficients of the polychlorinated biphenyls. *J. Phys. Chem. Ref. Data* **1986,** *15*, (2), 911-929.

12. Liu, L.; Wu, F.; Haderlein, S.; Grathwohl, P., Determination of the subcooled liquid solubilities of PAHs in partitioning batch experiments. *Geoscience Frontiers* **2013,** *4*, (1), 123-126.

13. Abraham, M. H.; Al-Hussaini, A. J., Solvation parameters for the 209 PCBs: Calculation of physicochemical properties. *J. Environ. Monit.* **2005,** *7*, (4), 295-301.

14. Zhao, Q.; Yang, K.; Li, W.; Xing, B. S., Concentration-dependent polyparameter linear free energy relationships to predict organic compound sorption on carbon nanotubes. *Scientific Reports* **2014,** *4*, 3888.

15. Apul, O. G.; Wang, Q. L.; Shao, T.; Rieck, J. R.; Karanfil, T., Predictive model development for adsorption of aromatic contaminants by multi-walled carbon nanotubes. *Environ. Sci. Technol.* **2013,** *47*, (5), 2295-2303.

16. Poole, S. K.; Poole, C. F., Retention of neutral organic compounds from solution on carbon adsorbents. *Anal. Commun.* **1997,** *34*, (9), 247-251.

17. Luehrs, D. C.; Hickey, J. P.; Nilsen, P. E.; Godbole, K. A.; Rogers, T. N., Linear solvation energy relationship of the limiting partition coefficient of organic solutes between water and activated carbon. *Environ. Sci. Technol.* **1996,** *30*, (1), 143-152.

18. Kamlet, M. J.; Doherty, R. M.; Abraham, M. H.; Taft, R. W., Linear solvation energy relationships .33. An analysis of the factors that influence adsorption of organic-compounds on activated carbon. *Carbon* **1985,** *23*, (5), 549-554.

19. Huang, W. L.; Young, T. M.; Schlautman, M. A.; Yu, H.; Weber, W. J., A distributed reactivity model for sorption by soils and sediments .9. General isotherm nonlinearity and applicability of the dual reactive domain model. *Environ. Sci. Technol.* **1997,** *31*, (6), 1703-1710.

20. Accardi-Dey, A.; Gschwend, P. M., Reinterpreting literature sorption data considering both absorption into organic carbon and adsorption onto black carbon. *Environ. Sci. Technol.* **2003,** *37*, (1), 99-106.

21. Accardi-Dey, A.; Gschwend, P. M., Assessing the combined roles of natural organic matter and black carbon as sorbents in sediments. *Environ. Sci. Technol.* **2002,** *36*, (1), 21-29.

22. Lohmann, R.; MacFarlane, J. K.; Gschwend, P. M., Importance of black carbon to sorption of native PAHs, PCBs, and PCDDs in Boston and New York harbor sediments. *Environ. Sci. Technol.* **2005,** *39*, (1), 141-8.